# Current singularities at finitely compressible three-dimensional magnetic null points

D. I. Pontin[a] and I. J. D. Craig
*Department of Mathematics, University of Waikato, Private Bag 3105, Hamilton, New Zealand*

(Received 29 March 2005; accepted 8 June 2005; published online 15 July 2005)

The formation of current singularities at line-tied two- and three-dimensional (2D and 3D, respectively) magnetic null points in a nonresistive magnetohydrodynamic environment is explored. It is shown that, despite the different separatrix structures of 2D and 3D null points, current singularities may be initiated in a formally equivalent manner. This is true no matter whether the collapse is triggered by flux imbalance within closed, line-tied null points or driven by externally imposed velocity fields in open, incompressible geometries. A Lagrangian numerical code is used to investigate the finite amplitude perturbations that lead to singular current sheets in collapsing 2D and 3D null points. The form of the singular current distribution is analyzed as a function of the spatial anisotropy of the null point, and the effects of finite gas pressure are quantified. It is pointed out that the pressure force, while never stopping the formation of the singularity, significantly alters the morphology of the current distribution as well as dramatically weakening its strength. The impact of these findings on 2D and 3D magnetic reconnection models is discussed. © *2005 American Institute of Physics*. [DOI: 10.1063/1.1987379]

## I. INTRODUCTION

Magnetic reconnection is a fundamental process of energy release in many areas of plasma physics. Yet for reconnection to be effective in weakly resistive astrophysical plasmas, strong localized currents must develop involving sharp gradients of the magnetic field. More generally, the plasma evolution is close to ideal, the magnetic field being effectively "frozen into" the plasma. A major aim of reconnection theory therefore, is to identify physical mechanisms which allow near-singular current structures to evolve from large scale field disturbances. Such mechanisms are believed to be important in the problem of quiescent coronal heating, as well as the rapid energy release of the solar flare (e.g., Ref. 1).

Historically, a great deal of work has been focused on the properties of two-dimensional (2D) magnetic *X*-points. It is well known theoretically that accumulated stresses in nonresistive plasmas can lead to localized current singularities—current sheets—in the weak field regions at the center of the *X*. For real plasmas, such small length scales signal the onset of resistive effects, in particular magnetic diffusion and reconnection. In addition, it seems the strength of the ideal singularity can provide a useful indicator for the rate of the energy release. What is less well understood is the part that finite plasma pressure may play in halting the collapse to singularity. Recent studies[2] suggest that while the pressure does not inhibit the singularity entirely, it may reduce its strength, effectively precluding strong, flarelike energy release (see also Ref. 3).

The situation is more complicated in three dimensions, where magnetic reconnection may occur at null points, or in their absence (e.g., Ref. 4)—for example, in the presence of closed field lines,[5] or, considered locally, at a 2D *X*-point threaded by some perpendicular, nonreconnecting field component.[6] In this paper, however, we will concentrate only on null point reconnection, in either "open" incompressible geometries or, in particular, in closed line-tied volumes. A key point is that the topological structure of magnetic null points in 2D and 3D is fundamentally different. At a 2D *X*-point, the separatrices—lines or surfaces that isolate topologically distinct flux regions—are the two pairs of magnetic field lines which begin or end at the null. In 3D, however, the skeleton of the null comprises a "spine" line and a "fan" surface. The spine is defined by the pair of field lines which enter (leave) the null from opposite sides, whereas the fan is formed by a family of field lines which extend out of (into) the null. In 3D therefore, there is an inherent asymmetry between the two separatrices. Locally, at a simple potential null point, the field lines in the fan are radial, and the spine and fan surface are perpendicular to one another. This structure changes significantly when currents are present at the null (see, e.g., Ref. 5 or for a mathematical formalism Ref. 7).

As in 2D, numerical evidence suggests that when a global 3D magnetic field is stressed, the current accumulates at null points (e.g., Ref. 8). However, the identification of 3D nulls as important sites of magnetic reconnection in plasmas is not universally accepted, and often the basic magnetic field topology associated with 3D reconnection is simply a planar current sheet threaded by an axial field component. Even if we assume that 3D nulls are of fundamental importance, it is far from clear that 3D null point reconnection can be understood in the same terms as reconnection at 2D *X*-points.

The aim of the present work is to treat 2D and 3D null point reconnection on the same footing by considering the collapse to singularity of line-tied magnetic null points, in

[a]Electronic mail: dpontin@math.waikato.ac.nz

 

compressible plasmas, in response to large scale magnetic disturbances. Our central point is that current structures associated with reconnection can be understood in terms of the focusing of externally generated large scale stresses in the field, no matter whether the geometry is two or three dimensional. However, we also explore the extent to which gas pressure can weaken the ideal collapse in both 2D and 3D geometries.

We begin in Sec. II by discussing how reconnection induced by magnetic collapse in line-tied, compact *X*-points relates to "driven" field line merging in open (incompressible) geometries. In Sec. III we introduce a 3D Lagrangian code, which we then use to explore the singular current structures that derive from perturbed 2D and 3D null points. Section IV is concerned with quantifying the strength of the singularity as a function of the compressiblity of the gas. We summarize our findings in Sec. V.

## II. DRIVEN RECONNECTION VERSUS MAGNETIC COLLAPSE

### A. Driven null point reconnection

One time-honored approach to 2D reconnection assumes that near anti-parallel fields are driven together in an open incompressible geometry. Although we will later discuss the effects of the compressibility of the plasma, the problem of incompressible merging provides an illustrative example of the transition from 2D to 3D models.

The key ingredient in incompressible reconnection models, as typified by classical Sweet–Parker merging, is a strong advective flow which carries the magnetic field into a localized, high current, diffusion region. It is now recognized that reconnection solutions can be constructed by exploiting the close symmetry between the **v** and **B** fields in incompressible plasmas. In ideal fluids this symmetry is reflected by the simplified MHD equations provided by the Elsasser variables $\mathbf{v}\pm\mathbf{B}$. More generally, if **P** is a large scale equilibrium field and **Q** some suitable disturbance field, the construction

$$\begin{pmatrix}\mathbf{v}(\mathbf{r},t)\\ \mathbf{B}(\mathbf{r},t)\end{pmatrix}=\begin{pmatrix}\alpha\\ \gamma\end{pmatrix}\mathbf{P}(\mathbf{r})+\begin{pmatrix}\gamma/\alpha\\ 1\end{pmatrix}\mathbf{Q}(\mathbf{r},t) \tag{1}$$

admits exact 2D reconnection solutions.[9] In this case, we can take the 2D form with $\mathbf{P}=(y,-x,0)$ and $\mathbf{Q}=[0,q(x,t),0]$. The condition $|\alpha|>|\gamma|\geqslant 0$ ensures that the flow is strong enough to maintain a localized sheet current, but otherwise the superposition constants are arbitrary. It is worth remarking that the case $\gamma=0$ corresponds to the annihilation of straight field lines, as described by Sonnerup and Priest.[10] More generally ($|\gamma|>0$), curved field lines are reconnected at the neutral point, as in the model of Craig and Henton.[9] Furthermore, a natural extension is also possible to so-called $2\frac{1}{2}$-dimensional models, where the magnetic field is three dimensional, but depends on only two spatial coordinates (see, e.g., Ref. 11). Solutions for the reconnection field **Q** may be transient or steady state but all known analytic solutions involve only one-dimensional forms for the disturbance field.

More important in the present context, is the simple transition from 2D to 3D solutions in the driven null point reconnection problem. In fact we need only identify **P** as a 3D background field, for example, the potential field

$$\mathbf{P}(x,y,z)=[\kappa x,(1-\kappa)y,-z], \tag{2}$$

to achieve 3D reconnection solutions.[12] In this case analytic solutions can be constructed with one-or two-dimensional disturbance fields. Two-dimensional merging is recovered by taking either $\kappa=0$ or $\kappa=1$—and reducing the dimensionality of the disturbance field.

### B. The *X*-point collapse in 2D

Even in two dimensions, a distinction should be drawn between reconnection driven by an externally imposed velocity field, as discussed above, and reconnection arising from an implosive collapse of the magnetic field. In contrast to the open geometry of the driven reconnection problem, the implosive collapse is most simply realized in a closed *X*-point plasma of negligible gas pressure which is nonresistively damped in some manner.

Consider a 2D potential *X*-point field $\mathbf{B}_0$ in a line-tied box, whose topology is changed by some disturbance **b**, according to

$$\mathbf{B}(\mathbf{r},t)=\mathbf{B}_0(\mathbf{r})+\mathbf{b}(\mathbf{r},t), \tag{3}$$

where $\mathbf{r}=(x,y)$ (say). As the field evolves in response to the initial Lorentz forces, fluid motions develop and these are eventually damped, removing kinetic energy from the plasma. However, because the evolution preserves the topology, only a singular equilibrium can be achieved by the relaxation—typically a *Y*-type current sheet in which the current density is infinite at points of vanishing **B**.[13,14]

Of course, when resistivity ($\eta$) is introduced into the problem, the singular collapse is arrested. In this case a strongly dissipating current layer forms whose thickness is governed by the resistivity but whose length is determined—as in the ideal evolution—by the amplitude of the disturbance field $|\mathbf{b}|$.

Can 2D collapse models provide fast reconnection? This requires that the rate of flux transfer, taken at the null point, should not scale as any positive power of resistivity, that is

$$\eta|\nabla\times\mathbf{B}|_n\sim\eta^0. \tag{4}$$

Studies[15–17] have shown that if resistivity provides *the sole damping mechanism*, then the reconnection rate depends, at most, logarithmically on the plasma resistivity. But the rate is slowed by the presence of axial field components and the effects of finite gas pressure.[3] In the simulations of compressible collapse described below we take $\eta=0$, and the small length scale which limits the magnitude of the current density is the numerical resolution. The connection between the scaling we obtain and the conditions for fast reconnection is discussed in Sec. IV C.

A further key question presents itself: is there an analogue of the 2D *X*-point collapse in three dimensions, as in the driven reconnection problem (discussed in Sec. II A)? It could be argued that the change in separatrix structure with

the dimensionality of the null makes the 2D and 3D collapse problems fundamentally different. In the remainder of this paper we challange this view by showing explicitly that null point collapse in 2D and 3D can be treated formally identically, in much the same way as the flow-driven reconnection problem. We shall discuss (i) how to initiate the collapse, (ii) the qualitative features of the current singularity, and (iii) the scaling of the current density in the vicinity of the neutral point.

### C. Initiation of collapse in 2D and 3D

Consider a potential null point located at the center of the volume $-1 \leqslant x,y,z \leqslant 1$. In 2D we initiate a collapse by adding a so-called "reconnective" disturbance field to the background potential field. Taking, for example, the configuration of Ref. 2, we have

$$\mathbf{B}_0 = B_0(y,-x), \tag{5}$$

$$\mathbf{b} = b_0(y(1-x^2),-x(1-y^2)), \tag{6}$$

where $B_0$ and $b_0$ are constant ($B_0 \gg b_0$). The disturbance field creates a mismatch between the amount of flux in adjoining lobes of the $X$-point. This can be seen by noting that the disturbance field lines have a circular topology, and so the superposition of $\mathbf{b}$ reinforces or cancels the background field ($\mathbf{B}_0$) in adjacent lobes of the $X$-point.

More specifically, the flux function for the initial field is given by

$$\psi(x,y) = B_0 xy + \frac{b_0}{2}(1-x^2)(1-y^2). \tag{7}$$

The effect of the disturbance field is to close up the separatrices—the lines defined by $\psi = b_0/2$—through the angle

$$\tan(\theta) = \frac{b_0}{2B_0}. \tag{8}$$

The disturbance introduces a Lorentz force which drives an implosion that collapses the field.

It is possible to set up an exactly analogous experiment in 3D. Consider, for example,

$$\mathbf{B}_0 = B_0(\kappa x,(1-\kappa)y,-z), \tag{9}$$

$$\mathbf{b} = b_0(0,-z,0), \tag{10}$$

where $B_0$ and $b_0$ are constant, and $\kappa$ is the anisotropy of the field ($0 \leqslant \kappa \leqslant 1$, say). As in the 2D case, it can be seen that, in any $yz$-plane, there is a reinforcement and canceling of the two fields ($\mathbf{B}_0$ and $\mathbf{b}$) in adjacent quadrants. The perturbed magnetic field is no longer in equilibrium, and the spine and fan are no longer perpendicular, as shown in Fig. 1(a) (cf. the kinematic reconnection of Ref. 18). In particular, the field line equations, namely

$$zx^{1/\kappa} = C_1, \quad yz^{(1-\kappa)} - \frac{b_0 z^{(2-\kappa)}}{(2-\kappa)B_0} = C_2, \tag{11}$$

can be used to show that the spine is tilted (in the $x=0$ plane) through the angle

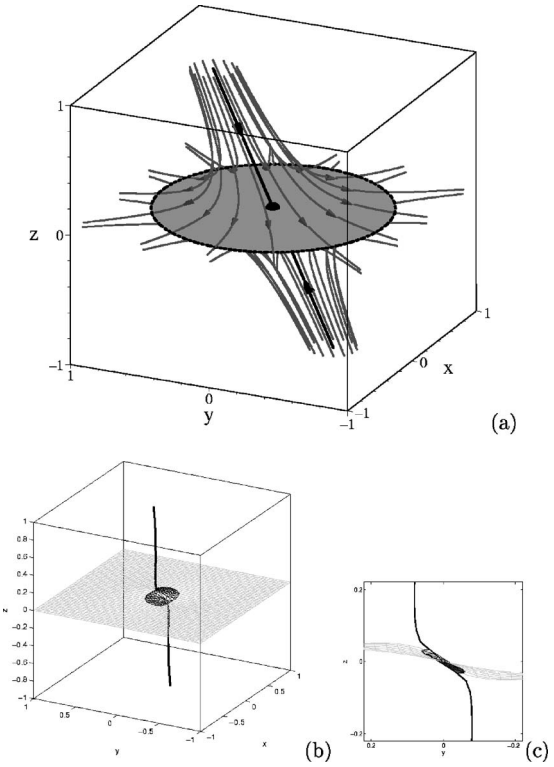


FIG. 1. (a) Schematic of the perturbed null point given by Eqs. (9) and (10); the black field line is the spine, and the gray disk represents the orientation of the fan plane. (b) Isosurface of the current magnitude at $J_{max}/3$, for the 3D null point collapse, with $\kappa=1/2$, $N=30$, $\beta=0.01$. The black line is the spine, and the gray grid represents the fan plane, and (c) a close-up in the $yz$-plane.

$$\tan(\theta) = \frac{b_0}{(2-\kappa)B_0}. \tag{12}$$

The resultant Lorentz force implodes the plasma, leading to a current singularity.

The collapsed current structure of the 3D $X$-point is illustrated in Fig. 1(b). The numerical scheme used to relax the field is detailed below. For the present we note that the current isosurface of the final relaxed state provides clear evidence that distortions of the spine lead to current accumulations in the vicinity of the null point. Figure 1(c) shows a close-up view of the current concentration in the $yz$-plane, demonstrating a similar structure to the Y-type current sheet of the 2D null collapse.

## III. COMPUTATION OF SINGULARITIES IN 2D AND 3D

### A. The Lagrangian relaxation scheme

We use a 3D relaxation scheme (as described in Ref. 19), which takes advantage of the fact that, due to the frozen-in field condition, the evolution of the vector $\mathbf{B}/\rho$ behaves in exactly the same way as the line element $\delta\mathbf{x}$ that joins two Lagrangian fluid particles. That is,

$$\frac{D}{Dt}\left(\frac{\mathbf{B}}{\rho}\right) = \left(\frac{\mathbf{B}}{\rho}\cdot\nabla\right)\mathbf{v}, \tag{13}$$

where $D/Dt$ denotes the material derivative, and $\rho$ is the mass density. Thus, if $\mathbf{X}=\mathbf{x}(t=0)$ denotes the initial position

of a fluid particle, then $\rho$ can be computed [in terms of $\rho_0 = \rho(t=0)$] using the Jacobian transformation

$$\rho = \left| \frac{\partial \mathbf{x}}{\partial \mathbf{X}} \right|^{-1} \rho_0, \tag{14}$$

assuming $\mathbf{x}(t)$ is known. It is the momentum equation, namely

$$\rho \frac{D\mathbf{v}}{Dt} = \mathbf{J} \times \mathbf{B} - \nabla P + \mathbf{F}, \tag{15}$$

where $\mathbf{J} = (\nabla \times \mathbf{B})$ is the dimensionless current density and $\mathbf{F}$ is some damping force, that determines the evolution of the fluid particles. The order of magnitude ratio of the second to the first terms on the right-hand side of Eq. (15) is known as the plasma beta ($\beta$), and indicates the relative importance of the Lorentz and plasma pressure forces. In what follows we shall use

$$P = \beta \rho^{\gamma}, \tag{16}$$

where $\gamma \sim O(1)$, to model the plasma pressure.

Consider now the form of the damping term $\mathbf{F}$. If $\mathbf{F}$ were not present, then the system would have no means of reducing its energy, and so would simply oscillate indefinitely, exchanging kinetic and magnetic energy. The conventional approach to damp these oscillations would be to use a traditional viscous force, to dissipate the kinetic energy of the system. Such an approach provides, at any given time, some "snapshot" of the evolution to the relaxed state. Since we are only interested in the final equilibrium configuration, and not in the evolution to it, we choose instead to determine the fully relaxed state using a fictitious damping force, of the form $\mathbf{F} = -F_0 \mathbf{v}$ (where $F_0 > 0$), that neglects the plasma inertia. Such a choice has the advantage of eliminating the wave properties of the plasma while guaranteeing a monotonic decay of the total energy. Moreover, it can be shown that the path taken in the relaxation affects neither the final equilibrium attained nor its stability properties.[19,20]

In practice, therefore, fluid particles defined on the initial mesh $-1 \leqslant x, y, z \leqslant 1$ and fixed on the boundaries, are evolved using the "frictional" form of the momentum equation. The magnetic flux, magnetic helicity, and $\nabla \cdot \mathbf{B}$ are automatically conserved in the relaxation. Thus, if the initial magnetic field satisfies $\nabla \cdot \mathbf{B} = 0$, this will always remain satisfied. The scheme is implicit and unconditionally stable, meaning that the computational cost of the simulations need not be prohibitive.

### B. Signatures of singular equilibria

Suppose an attempt is made to compute the singular current structures that derive from the collapse of the initial fields of Sec. II C. We expect that, although local quantities such as the current density at the null may diverge with resolution, integrated quantities should remain well defined. We therefore examine the dependence of the current density at the null on the numerical resolution. On the basis of previous studies it is expected that the divergence should take the form

$$J_{max} \simeq J_0 N^{\mu}, \tag{17}$$

where $N$ defines the initial $\mathbf{x}$-mesh spacing according to $\Delta x = \Delta y = \Delta z = 1/N$. The exponent $\mu > 0$ provides a measure of the strength of the current singularity. If gas pressure weakens the singularity then $\mu$ should decline with increasing plasma $\beta$.

We also calculate the total current

$$I_N = \int \mathbf{J} \cdot \mathbf{dS} \tag{18}$$

through a plane passing through the null point, perpendicular to the current orientation at the null. Even though the peak current diverges, the integrated current of the collapsed field should be approximately constant with resolution, since this may be determined by a line integral (Ampère's law) over the strong outer field regions, which are far from the current buildup, and thus largely controlled by the line-tied boundaries.

### C. Computational setup

In order to drive a singularity in the 2D case, we need only maintain a relative displacement of one or other of the separatrices between the null point and the boundary (a "reconnective" disturbance). It is less clear what types of perturbation will cause a collapse to singularity of the 3D null point. To investigate this in practice, it is simplest to leave the initial 3D null point field undisturbed, and to introduce displacements of the boundaries, using some combination of rotation and shear. Subject to this restriction, the boundary displacements are extended linearly into the interior of the computational domain.

Any disturbance which is to change the topology of the magnetic field requires a sustained perturbation of the separatrices, i.e., one which is maintained by the boundary line-tying. Any such disturbance can be decomposed into a rotation plus a translation. We find that any rotation, of the fan plane or about the spine, leads to current concentrations in the vicinity of the null separatrices, but concentrated at the boundaries of the domain near the driving footpoints. By contrast, a shear of one or both of the separatrices results in the formation of a current concentration at the null itself. In what follows, we consider a shear of the spine axis, in the manner of Sec. II C, although shearing the fan is entirely equivalent. The crucial characteristic, as in 2D, is that the separatrices are closed up from the orthogonal configuration, as in Fig. 1.

We begin by describing the results of two specific sets of simulations, in each of which the initial magnetic field is given by Eq. (9). In one set of simulations, we set $\kappa = 1/2$ to give an isotropic 3D null, while in the other we set $\kappa = 0$ to give a 2D null point (in all $yz$-planes). We now apply an initial perturbation to the Lagrangian mesh in the $y$-direction, in the form of a localized shear:

$$p_y = p_0 f(x) \tfrac{1}{2}[1 + \cos(\pi y)] z, \tag{19}$$

where $p_0$ is a constant. The only difference between the 2D ($\kappa = 0$) and 3D ($\kappa = 1/2$) simulations is that for the 3D null

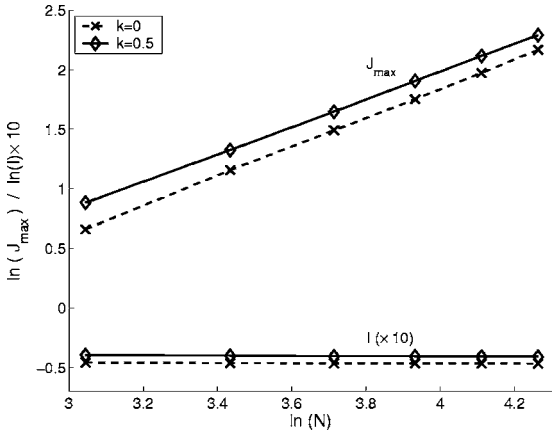


FIG. 2. Logarithmic scaling of peak current ($J_{max}$) and integrated current ($I$) (multiplied by 10 for clarity) with resolution ($N$), for the 2D (dashed line) and 3D (solid line) null points.

we let $f(x)=\frac{1}{2}[1+\cos(\pi x)]$, so that we have a local shear of the spine axis, in opposite directions above and below the fan ($z=0$) plane. However, since the 2D null point field is independent of $x$, it is more appropriate in this case to use $f(x)=1$, giving a shear of one separatrix which is independent of the invariant coordinate direction, $x$.

Note that the perturbation maintains the dimensions of the box, falling to zero at $x=y=\pm 1$, but is held on by the boundary line-tying on $z=\pm 1$, and that we choose $p_0=0.1$. In what follows the relaxation of the perturbed field is terminated when the initial forces, typically of order unity, have been reduced by a factor of approximately $10^4$.

### D. 2D and 3D relaxation results

The 2D relaxation simulation, with $\kappa=0$, proceeds as expected, with a localized current concentration developing, centered on the null point. The peak current for runs of different resolution is plotted in Fig. 2. In a strictly one-dimensional current sheet collapse (with $\beta=0$) it can be shown analytically that we expect the peak current ($J_{max}$) to scale as $N^2$ (see, e.g., Ref. 21). A logarithmic plot of $J_{max}$ versus $N$ confirms that that the peak current follows a power law scaling of the form of Eq. (17). For finite $\beta$ we generally find $0<\mu<2$, but the systematic increase with resolution remains in sharp contrast to the constancy of the integrated current (in the $yz$-plane through the null).

In the 3D ($\kappa=1/2$) simulation, a current concentration which is peaked at the null also develops, as described previously. The peak and integrated current ($J_{max}$ and $I_N$) for the 3D null are also plotted in Fig. 2, and show a remarkably similar scaling to those for the 2D null, again giving the expected signatures of a singularity. This time the integrated current is calculated through the surface $x=0$, since $J_x$ makes the dominant contribution to **J**. In Fig. 1(b) a typical current isosurface (at $J_{max}/3$) is plotted, together with the spine and fan of the null point, from which it is evident that the current is centered on the null.

It is interesting to note that there are also morphological similarities between the 3D current sheet and the familiar 2D picture. In Fig. 1(c), a close-up of the current concentration is shown, in the plane of the shear ($yz$-plane). Noticably the fan and spine have collapsed toward each other locally and, along with the current sheet, approximate the Y-type configuartion expected in a 2D null collapse. Further insight into the singular current structure may be gained by examining the profile of the current modulus in the vicinity of the null, displayed in Figs. 3(a)–3(c). It is apparent that the current profile is nondifferentiable at the null in every direction. This

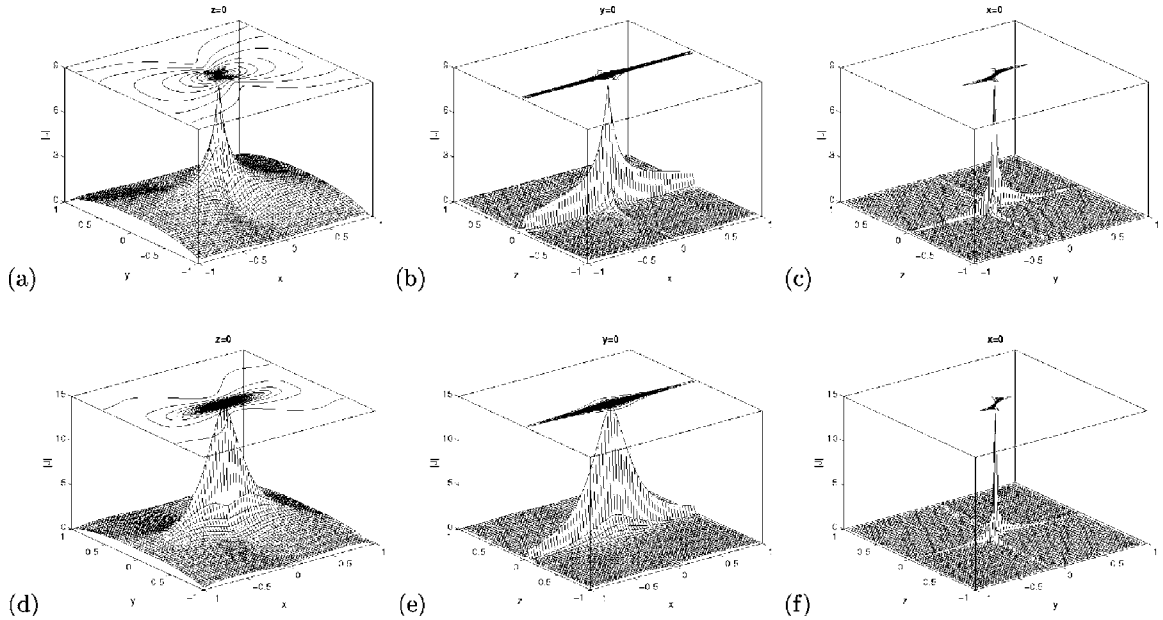


FIG. 3. Plots of $|J|$ for the isotropic ($\kappa=1/2$) 3D null in the (a) $xy$-plane, (b) $xz$-plane and (c) $yz$-plane, for $N=30$ and $\beta=0.01$. Overlayed on the top of the domain in each case is a contour plot of $|J|$, with the same contour levels plotted in each frame. (d)–(f) The same plots for an anisotropic null with $\kappa=1/4$.

suggests that, at least in the case of an isotropic null point ($\kappa=1/2$), the current density forms a singular "spike" centered on the null.

### E. Dependence on isotropy ($\kappa$)

When the background null point is no longer isotropic the current singularity assumes a more "sheetlike" character. That is, in the case of a 3D null with $\kappa \neq 1/2$, the current in the relaxed state preferentially spreads out along the direction of weak field in the fan plane. As is shown in Figs. 3(d)–3(f) for $\kappa=1/4$ and $\beta=0.01$, this can lead, for sufficiently high anisotropy and/or $\beta$, to a current profile which is considerably less peaked in the weak field direction, such that the current profile is no longer nondifferentiable along this direction. It appears that in this case there is present a two-dimensional current "sheet" rather than a 3D-singular "spike."

### F. Summary

We have confirmed by direct computation that the 2D and 3D magnetic collapse problems can be treated in a formally equivalent manner. Although the perturbation of 3D nulls is far less well-studied than the analogous problem in 2D, the essential features of a reconnective disturbance remain the same in that the disturbance introduces currents by distorting the sepratrices of the equilibrium field. Such currents eventually accumulate at the null producing well-defined singularties in the field.

It is interesting to compare the present results with those of Rickard and Titov[22] who consider linearized perturbations of the cold, resistive magnetohydrodynamic equations via a modal analysis in cylindrical geometry. They assert that all local perturbations to a 3D null point which may generate current at the null itself are of the form of either an $m=0$ mode or an $m=1$ mode, or some combination thereof. They find that $m=0$ mode disturbances lead to current concentrations at certain locations along the separatrices, while it is $m=1$ mode disturbances which lead to currents which focus at the null itself. We find here that the long-term behavior of such perturbations is similar. As discussed previously, rotations ($m=0$) lead in our case only to diffuse currents near the driving footpoints. This suggests that—not only in the short term (as in Ref. 22), but also as the relaxation progresses—rotational disturbances are not strongly attracted to the null point. In contrast, persistant shear, anchored by line-tying, results in well-defined current singularities at the null.

## IV. EFFECT OF COMPRESSIBILITY

In this section, we consider the effect that the plasma pressure has on the current growth at the null point. It can be shown (see, e.g., Ref. 2) that in a strictly one-dimensional configuration, a finite plasma pressure stalls the collapse to singularity. This is not true in higher-dimensional problems—because the Lorentz force is no longer constrained to be irrotational—but the strength of the singularity is considerably reduced, as confirmed by the Eulerian 2D calculations of Ref. 2. Below we briefly verify the 2D results, before going on to compare with the 3D null.

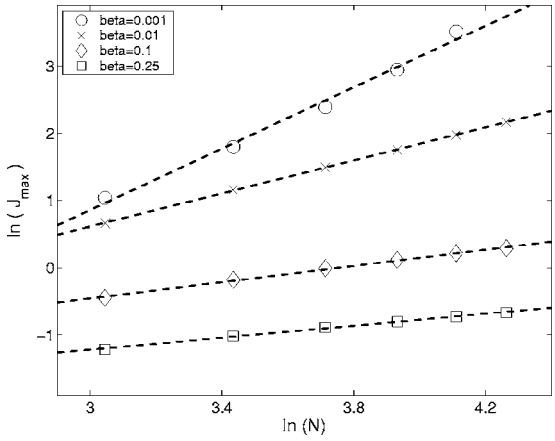


FIG. 4. Scaling of peak current ($J_{max}$) with resolution ($N$) for various values of the plasma $\beta$ for the 2D null. The dashed lines give best fits via linear regression to the data points.

### A. 2D null

In order to investigate the effect of the pressure force, the simulations described in the previous section were repeated for various different values of the parameter $\beta$. These calculations differ from those of Ref. 2 in that here we use a Lagrangian rather than an Eulerian mesh. The analytic idealization of vanishing plasma pressure ($\beta=0$) is not well defined computationally since only "finite" mesh deformations are permissible. Although in general the magnetic pressure is also expected to inhibit compression (perpendicular to **B**), it is not sufficient to prevent the coalescence of fluid elements along the field. What this implies computationally is that the zero $\beta$ limit must be approximated by some small $\beta$, typically $\beta \leqslant 10^{-3}$.

Figure 4 confirms that the singularity weakens, i.e., the index $\mu$ [see Eq. (17)] decreases, as the plasma beta increases. The dashed lines on the plot are best-fit lines calculated by a simple linear regression, and give the scalings in the first column of Table I. Note that the scaling of $J_{max} \sim N^{2.28}$ when $\beta=10^{-3}$ compares closely with the theoretical prediction for the 1D collapse with $\beta=0$ [$J_{max} \sim N^2$ (Ref. 21)]. However, while the scaling for the other values of $\beta$ is remarkably well adhered to, for this low value of $\beta$ the relationship is not exactly linear, with the scaling appearing to accelerate for large $N$. Probably not too much should be read into this effect since the convergence of the computation

TABLE I. Values of the power law scaling index $\mu$ for various values of $\kappa$ and $\beta$.

| $\beta$ | $\mu:\kappa=0$ | $\mu:\kappa=\frac{1}{4}$ | $\mu:\kappa=\frac{1}{2}$ |
|---|---|---|---|
| 0.001 | 2.35 | 2.56 | 2.28 |
| 0.01 | 1.16 | 1.40 | 1.23 |
| 0.1 | 0.62 | 0.60 | 0.61 |
| 0.25 | 0.53 | 0.45 | 0.45 |

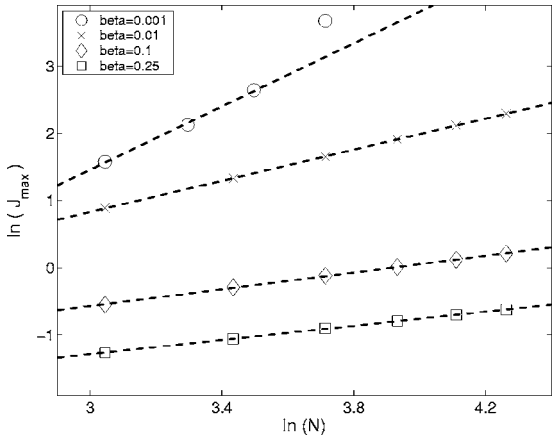


FIG. 5. Scaling of peak current ($J_{max}$) with resolution ($N$) for various values of the plasma $\beta$ for the 3D null. The dashed lines give best fits via linear regression to the data points.

becomes less assured for very high plasma compressions. What is noticable, however, is an effect mentioned in Ref. 2, namely the weaker localization of the current sheet, that accompanies the lower peak current at high $\beta$. That is, at fixed resolution $N$, the current tends to spread along the separatrices of the null, forming "wings" which adjoin the central current sheet.

### B. 3D null

The exact same analysis may now be performed in the case of the 3D null point. The resultant scalings of peak current versus resolution for the same values of $\beta$ (for $\kappa=1/2$) are shown in Fig. 5, and the index $\mu$ [see Eq. (17)] giving the slopes of the best-fit lines is displayed in the third column of Table I. The scaling behavior for the 3D null ($\kappa=1/2$) is remarkably similar to the 2D computation ($\kappa=0$), and in fact there is a smooth transition between the 2D and 3D collapse. We may take any value for the field anisotropy parameter $\kappa$ ($0\leqslant\kappa\leqslant 1$), with $\kappa=0$ simply being one special case. The scalings for $\kappa=1/4$ are given in the second column of Table I to illustrate this point. Aside from the suggestion of a slightly stronger singularity at low $\beta$, the intermediate $\beta$ values are consistent with previous computations.

In Fig. 6 we explore the extent to which the current density becomes less localized with increasing beta in the 3D collapse. By plotting isosurfaces at different current levels, we can see that such spreading does indeed occur, the current concentration taking on a disk-type structure [as in Fig. 1(b)]. We have applied various different types of shearing perturbations to the null point, disturbing the spine and/or fan, and it appears that the current is more prone to spreading in the fan plane in each case, although the effect is also seen to a lesser extent along the spine. This is demonstrated in Fig. 6(a), where the current in the $x=0$ plane is plotted, from which it is evident that current "wings" are present along the $y$-direction and to a lesser extent along the spine ($z$-) axis. Furthermore, in the isotropic $\kappa=1/2$ case, there is preferential spreading along the direction perpendicular to the shear, as the field near the fan "buckles" along this direction to take up the stress. This is illustrated in Figs. 6(b) and 6(c), where

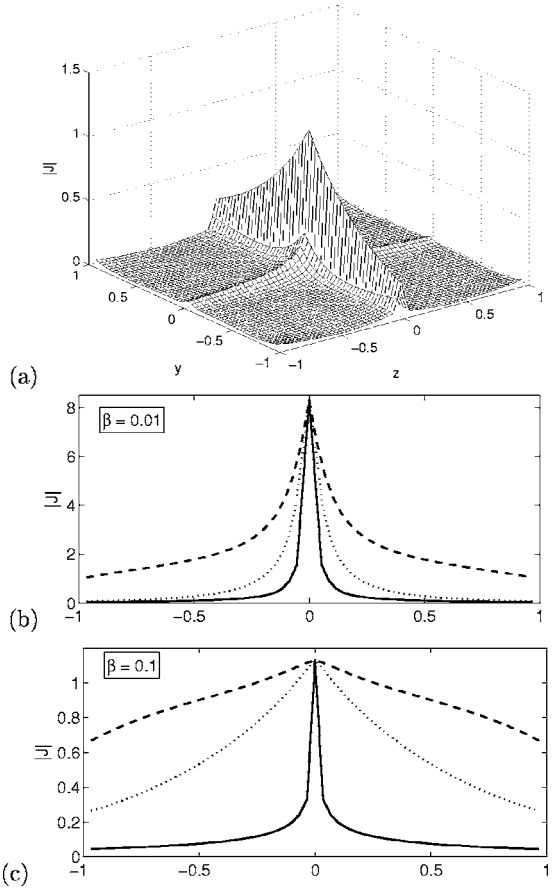


FIG. 6. (a) Modulus of the current plotted in the $x=0$ plane demonstrating the spreading along the spine and fan, for $N=30$, $\kappa=1/2$ and $\beta=0.1$. (b), (c) Current modulus along the spine (solid line) and along the $x$ (dashed) and $y$ (dotted) directions in the fan plane, showing the spreading of the current sheet, for (b) $\beta=0.01$ and (c) $\beta=0.1$.

the current magnitude along the spine, and in the fan in the $x$- and $y$-directions, is plotted. The current profile is clearly broader in the $x$-direction, but also in general the current sheet extends more in the fan than along the spine, with the effect being more pronounced for larger $\beta$, as expected.

Note finally that for $\kappa=1/4$, the preferential spreading is always in the weak field direction, regardless of the direction (in $xy$) of the shear. The least significant spreading of all is still along the spine.

### C. The possibility of fast reconnection

As already mentioned, fast reconnection requires that the current density at the null point should scale as $\eta^{-1}$. Although the link between the current density scalings and the thickness of the resistive current layer must be carefully interpreted (see, e.g., Ref. 2), the fact that the singularity weakens with increasing gas pressure makes the condition for fast reconnection increasingly hard to achieve.

Note, for example, that in a quasi-1D Lagrangian collapse with zero gas pressure, the peak current density must scale as $N^2$ to achieve fast reconnection (see Ref. 2). This strong scaling was achieved in the present computations only for the lowest values of beta ($\beta\leqslant 10^{-3}$). For higher beta, the singularity weakens and the current density becomes more

diffuse. Since, in common with Craig and Litvinenko,[2] we know of no reconnection model which can maintain its speed against the weakening strength of the ideal singularity, the present results appear to militate against fast reconnection in finitely compressible plasmas.

## V. SUMMARY

In this study we have shown that reconnection associated with 3D nulls can be understood in much the same manner as classical 2D merging. This is true no matter whether the problem is formulated in terms of flow driven, incompressible merging, or as the collapse to singularity of compressible, line-tied *X*-points. Note that we do not assert that 3D reconnection is always associated with 3D null points—reconnection in three dimensions may also occur in 2D current sheets which are threaded by a perpendicular field component. What we do maintain is that there is a continual and systematic transition between the 2D and 3D null point formulations.

We began by noting that singularities at 3D null points can be induced in two ways, either by considering the addition of a perturbation field to a background equilibrium configuration, or by perturbing the initial equilibrium via plasma motions. The key ingredient in both cases is a sustained displacement of the magnetic separatrices. One approach to analyzing the collapsed state is to use magnetic relaxation methods to quantify the strength and morphology of the singularity. Integrated quantities in the final state should remain well defined but local quantities such as the peak current are expected to diverge systematically with numerical resolution $N$. Of central interest is how the strength of the singularity depends on the plasma beta ($\beta$) and on the isotropy ($\kappa$) of the background null point. Such questions can be investigated by exploring the rate of divergence of the peak current with resolution.

In two-dimensional simulations the singularity takes the form of a Y-type current sheet. In this case we confirmed, in line with Ref. 2, that finite pressure weakens but does not stall the singularity formation entirely. An identical approach was used for the 3D null point. It was found that translational perturbations of the null point separatrices were most effective in triggering a singular collapse. We demonstrated that the adjustment of the anisotropy parameter ($\kappa$) allowed a smooth transition between the 2D and 3D null point computations (see Sec. II C).

Turning now to the influence of plasma pressure, we found 3D current density scalings that closely match the 2D results. Once again, the isotropy paramater allows for a smooth interpolation between the 2D and 3D scalings. Noticeably, the morphology of the 3D current sheet changes appreciably when a nonzero $\beta$ is assumed. The current weakens as it spreads along the separatrices, preferentially in the plane of the fan. The scalings of the current density imply, as in the 2D problem, that fast reconnection can only be maintained in the limit of small gas pressures.

## ACKNOWLEDGMENT

This work was supported financially by the Marsden Fund (02-UOW-050 MIS).

[1] E. N. Parker, *Cosmical Magnetic Fields* (Clarendon, Oxford, 1979).
[2] I. J. D. Craig and Y. E. Litvinenko, Phys. Plasmas **12**, 032301 (2005).
[3] A. N. M. McClymont and I. J. D. Craig, Astrophys. J. **466**, 487 (1996).
[4] K. Schindler, M. Hesse, and J. Birn, J. Geophys. Res., [Space Phys.] **93**, 5547 (1988).
[5] Y. T. Lau and J. M. Finn, Astrophys. J. **350**, 672 (1990).
[6] E. R. Priest and P. Démoulin, J. Geophys. Res., [Space Phys.] **100**, 23443 (1995).
[7] C. E. Parnell, J. M. Smith, T. Neukirch, and E. R. Priest, Phys. Plasmas **3**, 759 (1996).
[8] K. Galsgaard and A. Nordlund, J. Geophys. Res., [Space Phys.] **102**, 231 (1997).
[9] I. J. D. Craig and S. M. Henton, Astrophys. J. **450**, 280 (1995).
[10] B. U. Ö. Sonnerup and E. R. Priest, J. Plasma Phys. **14**, 283 (1975).
[11] I. J. D. Craig, R. B. Fabling, S. M. Henton, and G. J. Rickard, Astrophys. J. Lett. **455**, L197 (1995).
[12] I. J. D. Craig and R. B. Fabling, Astrophys. J. **462**, 969 (1996).
[13] R. M. Green, in *IAU Symposium 22: Stellar and Solar Magnetic Fields* (North-Holland, Amsterdam, 1965), p. 398.
[14] S. I. Syrovatskii, Sov. Phys. JETP **33**, 933 (1971).
[15] I. J. D. Craig and A. N. M. McClymont, Astrophys. J. **371**, L41 (1991).
[16] I. J. D. Craig and A. N. M. McClymont, Astrophys. J. **405**, 207 (1993).
[17] A. B. Hassam, Astrophys. J. **399**, 159 (1992).
[18] D. I. Pontin, G. Hornig, and E. R. Priest, Geophys. Astrophys. Fluid Dyn. **99**, 77 (2005).
[19] I. J. D. Craig and A. D. Sneyd, Astrophys. J. **311**, 451 (1986).
[20] R. Chodura and A. Schlueter, J. Comput. Phys. **41**, 68 (1981).
[21] F. Ali and A. D. Sneyd, Sol. Phys. **205**, 279 (2002).
[22] G. J. Rickard and V. S. Titov, Astrophys. J. **472**, 840 (1996).